electronic reprint

Acta Crystallographica Section D
Biological Crystallography
ISSN 0907-4449
Editors: **E. N. Baker and Z. Dauter**

Interaction energies between glycopeptide antibiotics and substrates in complexes determined by X-ray crystallography: application of a theoretical databank of aspherical atoms and a symmetry-adapted perturbation theory-based set of interatomic potentials

Xue Li, Anatoliy V. Volkov, Krzysztof Szalewicz and Philip Coppens

Acta Crystallographica Section D
Biological Crystallography
ISSN 0907-4449

Interaction energies between glycopeptide antibiotics and substrates in complexes determined by X-ray crystallography: application of a theoretical databank of aspherical atoms and a symmetry-adapted perturbation theory-based set of interatomic potentials

Xue Li,[a] Anatoliy V. Volkov,[a] Krzysztof Szalewicz[b] and Philip Coppens[a]*

[a]Chemistry Department, State University of New York at Buffalo, Buffalo, NY 14260-3000, USA, and [b]Department of Physics and Astronomy, University of Delaware, Newark, Delaware 19716, USA

Correspondence e-mail: coppens@buffalo.edu

Received 6 March 2006
Accepted 10 April 2006

Intermolecular interaction energies between fragments of glycopeptide antibiotics and small peptide ligands are evaluated using geometries determined by X-ray crystallography and recently developed methods suitable for application to very large molecular complexes. The calculation of the electrostatic contributions is based on charge densities constructed with a databank of transferable aspherical atoms described by nucleus-centered spherical harmonic density functions [Volkov *et al.* (2004), *J. Phys. Chem.* **108**, 4283–4300], and uses the accurate and fast EPMM method [Volkov *et al.* (2004), *Chem. Phys. Lett.* **391**, 170–175]. Dispersion, induction and exchange-repulsion contributions are evaluated with atom–atom potentials fitted to intermolecular energies from SAPT (symmetry-adapted perturbation theory) calculations on a large number of molecules. For a number of the complexes, first-principle calculations using density functional theory have been performed for comparison. Results of the new methods agree within reasonable bounds with those from DFT calculations, while being obtained at a fraction (less than 1%) of the computer time. A strong dependence on the geometry of the interaction is found, even when the number of hydrogen bonds between the substrate and antibiotic fragment is the same. While high-resolution X-ray data are required to obtain interaction energies at a quantitative level, the techniques developed have potential for joint X-ray/energy refinement of macromolecular structures.

1. Introduction

Bacterial resistance to antibiotics is a major problem in our ability to overcome infectious disease. Since its discovery in 1956, the glycopeptide antibiotic vancomycin has been used worldwide as a last-resort antibiotic to treat infections by Gram-positive bacterial pathogens (McCormick *et al.*, 1955–1956; Harris *et al.*, 1983; Malabarba *et al.*, 1997). However, in 1987 vancomycin-resistant enterococci were reported in hospitals (Uttley *et al.*, 1988; Woodford *et al.*, 1995) and ten years later vancomycin resistance was observed in staphylococcal isolates (Hiramatsu, 1998). Vancomycin resistance in *Staphylococcus aureus* has also emerged and spread rapidly in the past two decades (Hiramatsu, 1998; Levy, 1998). As a consequence, the mechanism of the antibiotic's bactericidal action has attracted widespread attention.

Vancomycin is the prototype member of the family of glycopeptide antibiotics. All members of this family have a heptapeptide backbone, but show small structural variations

and differ in their glycosidation state. The hydrogen bonding of vancomycin to a number of small substrate molecules is illustrated in Fig. 1. Vancomycin inhibits normal cross-linking activity in the peptidoglycan of bacterial cell walls by binding to the dipeptide D-alanine-D-alanine (DADA) terminal of the peptidoglycan, which involves at least four hydrogen bonds. This prevents the transpeptidation reaction necessary for the biosynthesis of the peptidoglycan cell wall (Barna & Williams, 1984; Reynolds, 1989; Wright & Walsh, 1992; Walsh *et al.*, 1996; Ge *et al.*, 1999; Roper *et al.*, 2000). The most common form of bacterial resistance results from the replacement of the C-terminal residue of DADA to give the depsipeptide D-alanine-D-lactate (DADLac). DADLac differs from DADA by substitution of an ester O atom for the amide group of DADA. The concomitant loss of a hydrogen bond in the cell-wall antibiotic complex and other factors result in a three orders of magnitude reduction of vancomycin's affinity for its target.

As extensive structural information has recently become available, it is now possible to evaluate the strength of the antibiotic–substrate interactions and their modification by chemical substitution using computational techniques. In the current work, a newly developed method, applicable to the evaluation of interactions of large molecular entities with substrates, is tested and compared with quantum-mechanical calculations and molecular-mechanics results on the energies of interaction of fragments of vancomycin and related balhimycins with substrates.

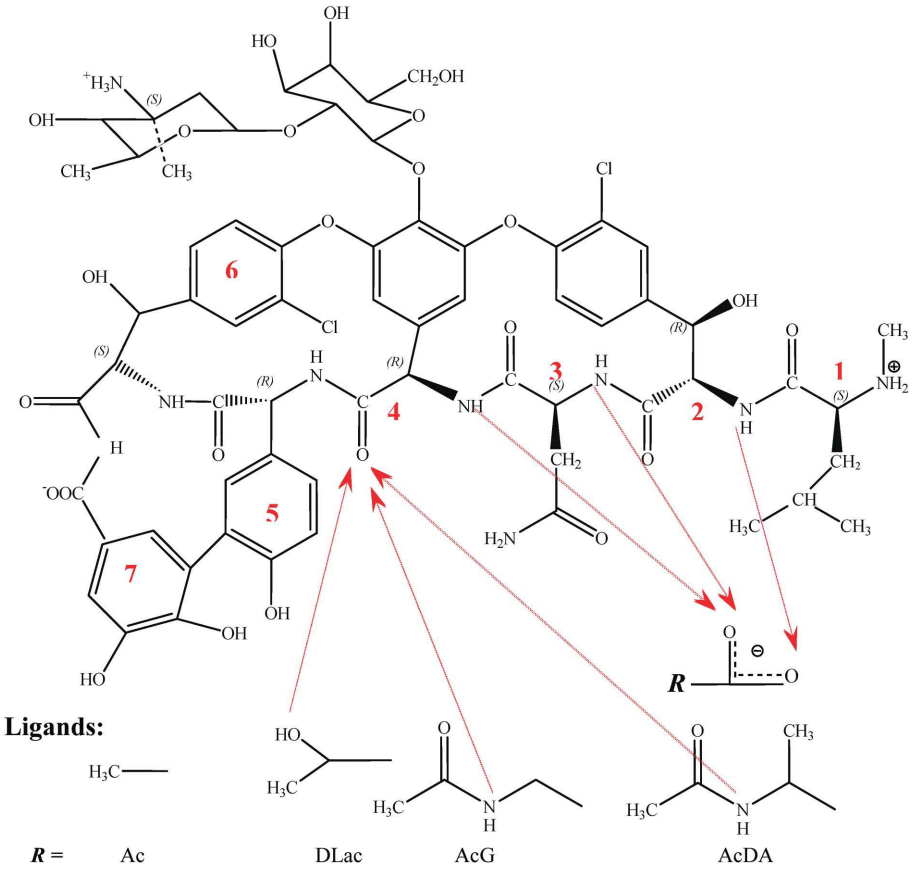

Figure 1
Schematic representation of vancomycin and its interactions with small ligands.

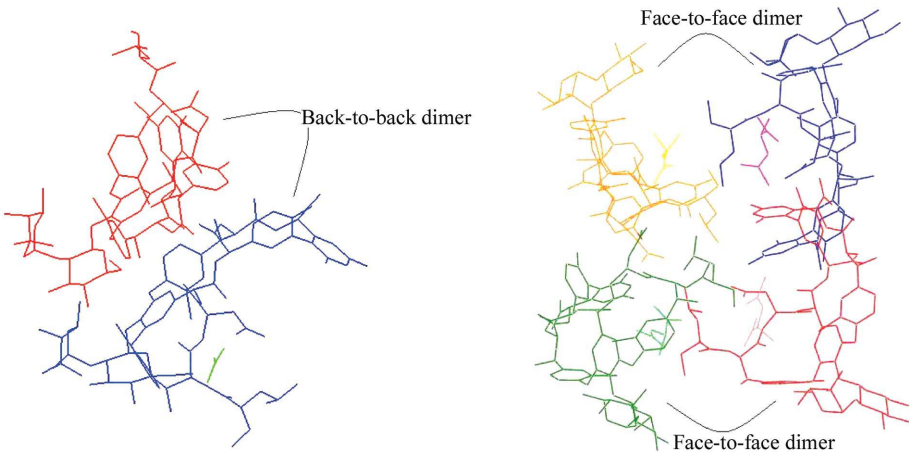

Figure 2
Illustration of the 'back-to back' dimer in vancomycin–Ac (green ligand) and the 'face-to-face' dimer in vancomycin–AcDA (purple, yellow, green and brown ligands).

2. Crystallographic information

The first X-ray structure determination of a vancomycin-related substance was reported in 1978 (Sheldrick *et al.*, 1978), while in 1995 Sheldrick and coworkers published the structure of the dimer of the glycopeptide ureidobalhimycin (Sheldrick *et al.*, 1995). In the latter structure, 'back-to-back' dimers ('back' being defined as the glucosidic side pointing away from the binding pocket) are stabilized by four hydrogen bonds between antiparallel polypeptide backbones. A year later, the crystal structures of vancomycin and the parvodicin aglycon became available (Schäfer *et al.*, 1996). The structure of the vancomycin–acetate (Ac) complex was solved by Loll in 1997 (PDB code 1aa5; Fig. 2*a*; Loll *et al.*, 1997). It identified for the first time the nature of the carboxylate recognition by vancomycin. Each vancomycin monomer binds an acetate ion through a hydrogen bond between one of the acetate O atoms and an amide proton of vancomycin residue 2 and O···H hydrogen bonds to the amide protons of residues 3 and 4 of the antibiotic, as illustrated schematically in Fig. 1, which also shows the interaction

Table 1
Binding constants reported in the literature (Loll *et al.*, 1999; Pearce *et al.*, 1995) and corresponding free-energy differences.

Ligand	Abbreviation	Affinity (M^{-1})	$\Delta\Delta G$† (kJ mol^{-1})
Acetate	Ac	30, 15	5.7, 7.4
N-Acetyl D-alanine	AcDA	300	‡
N-Acetyl glycine	AcG	80	3.3
D-Lactate	DLac	80	3.3

† From $\Delta\Delta G = \exp[-(K_2/K_1/RT)]$. ‡ Taken as reference value.

with other small-molecule substrates. The methyl group interacts with the aromatic ring of residue 4. There is no interaction between the side chain of asparagine (residue 3) and the ligand.

The complexes of D-lactate (DLac) and *N*-acetyl glycine (AcG) with vancomycin (PDB codes 1c0r and 1qd8; Loll *et al.*, 1999) are isomorphous with vancomycin–Ac. They crystallize in the same tetragonal space group $P4_32_12$, with almost identical unit-cell parameters. The two carboxylate O atoms of each ligand form the same three hydrogen bonds to the vancomycin backbone as in the vancomycin–Ac complex, whereas the positions of the other hydrogen bonds differ. The amide proton of AcG forms a hydrogen bond to the carbonyl O atom of residue 4 of the antibiotic. In the DLac complex, the hydroxyl group of DLac forms a hydrogen bond to the carbonyl O atom of residue 4 (Fig. 1).

The crystal structure of the complex of vancomycin with the cell-wall mimetic *N*-acetyl-D-alanine (AcDA) was reported in 1998 (Fig. 2*b*; Loll *et al.*, 1998). It contains 'back-to-back' dimers, but also a novel 'face-to-face' dimer between vancomycin and its symmetry equivalent. The bound AcDA ligands comprise a significant portion of the face-to-face dimer interface, suggesting that it will form only in the presence of ligands. Unlike the vancomycin back-to-back dimer in the low-affinity complexes, in which the dimer is bound to only one substrate molecule, all ligand-recognition pockets are ligand-occupied in the vancomycin AcDA complex, giving a 1:1 antibiotic:ligand ratio. The two types of dimer are illustrated in Fig. 2.

More recently, several atomic resolution structures were obtained of the related molecules balhimycin and deglucobalhimycin complexed with different peptide models of the nascent peptidoglycan (Lehmann *et al.*, 2002), including a balhimycin–tripeptide (L-Lys-DADA; PDB code 1go6) and a deglucobalhimycin–dipeptide (DADA) complex (PDB code 1hhu), which has four molecules of the antibiotic–dipeptide complex in the hexagonal asymmetric unit (Lehmann *et al.*, 2002). These complexes are further discussed in §5.2 below.

3. Previous studies on the strength of the antibiotic–substrate interaction

Only a few studies on the strength of the glycopeptide–substrate binding interaction have been reported to date. Molecular-dynamics calculations of the difference between the free energy of binding of the peptide AcDADA and the depsipeptide Ac-D-alanine-D-lactate (AcDADLac) with aglycovancomycin using a modified version of the *CHARMM*22 program gave a result of ∼20.5 kJ mol^{-1} (Axelsen & Li, 1998), whereas solution measurements of the relative affinities of vancomycin–small-ligand complexes give only small differences of 3.3–7.4 kJ mol^{-1} (Table 1; Li *et al.*, 1997). More recent theoretical calculations using both HF and DFT methods (the latter with the B3LYP hybrid functional) gave the differences in binding energy of AcDADA and AcDADLac to aglycovancomycin as 20.3 kJ mol^{-1} (HF) and 15.1 kJ mol^{-1} (DFT) (Lee *et al.*, 2004).

4. Methods used

4.1. Evaluation of the electrostatic interaction energy

In the Buckingham-type approximation (Buckingham, 1967; Stone, 1995; Coppens, 1997), which is valid for non-overlapping charge densities, the electrostatic interaction energy is expressed as a sum of interactions between spherical harmonic density functions (multipoles) centered on the atoms of the interacting molecules according to the expression

$$E_{\rm es} = \sum_{i}^{N_A}\sum_{j}^{N_B} T(\mathbf{r}_{ij})q_i q_j + T_\alpha(\mathbf{r}_{ij})(q_i\mu_{\alpha,j} - q_j\mu_{\alpha,i}) + T_{\alpha\beta}(\mathbf{r}_{ij})(\tfrac{1}{3}q_i\Theta_{\alpha\beta,i} + \tfrac{1}{3}q_j\Theta_{\alpha\beta,i} - \mu_{\alpha,j}\mu_{\alpha,j}) + \ldots, \quad (1)$$

where q, μ, Θ, ... are the permanent atomic moments (monopole, dipole, quadrupole *etc.*) of the atoms in the unperturbed molecular-charge distributions and the parameters $T_{\alpha\beta\gamma\ldots}(\mathbf{r}_{ij})$ are the so-called interaction tensors which depend on the separation of atomic centers $\mathbf{r}_{ij}$. The Einstein summation convention for the indices α, β, γ, ..., denoting the Cartesian coordinates, is implied in (2), and the parameters N_A and N_B represent the number of atoms in molecular fragments A and B, respectively.

The series converges quite rapidly when multipoles distributed over the atomic nuclei are used, but the expression is valid only for non-overlapping charge distributions.

The exact expression for the electrostatic energy is given by

$$E_{\rm es} = \sum_{\alpha\in A}\sum_{\beta\in B}\frac{Z_\alpha Z_\beta}{\gamma_{\alpha\beta}} - \int_A \rho_A(r)V_B^{\rm nuc}(r)\,{\rm d}^3r_A - \int_B \rho_B(r)V_A^{\rm nuc}(r)\,{\rm d}^3r_B + \int_A\int_B \frac{\rho_A(r_1)\rho_B(r_2)}{r_{12}}\,{\rm d}^3r_B\,{\rm d}^3r_A, \quad (2)$$

where ρ_A and ρ_B are the molecular electron densities, $V_A^{\rm nuc}$ and $V_B^{\rm nuc}$ are the nuclear potentials of molecules A and B, respectively, and $\gamma_{\alpha\beta}$ is the distance between nuclei α and β. In the EPMM method (Volkov, Koritsanszky *et al.*, 2004), the exact Coulomb integrals of (2) are evaluated using numerical (quadrature) methods for short-range atom–atom interactions, while the Buckingham-type expression (1) is retained for the more numerous interactions between atoms beyond a certain cutoff limit, which is typically set at 4.0 Å. The method results in an essentially exact evaluation of the electrostatic component of the interaction energy at a considerable saving in computation time compared with full evaluation of (2).

For application to large molecules, the charge density is constructed using a databank of transferable aspherical atomic densities, or 'pseudoatoms', derived from theoretical calculations on a large number of small molecules (Volkov, Li *et al.*, 2004; Volkov & Coppens, 2004). In the databank (DB) the atomic densities are expressed as a sum over atomic multipoles, in analogy with the model used in experimental charge-density analysis (Hansen & Coppens, 1978). As described in the reference, the databank is based on single-point calculations on selected small molecules performed with the *Gaussian*98 program at the density functional level of theory (DFT), using a standard split-valence double-exponential 6-31G** basis set. In the current study, the DB+EPMM results for a number of complexes are compared with those from first-principle theoretical calculations, which are described in §4.4.

4.2. The MMFF94 force-field calculations

Molecular-mechanics calculations were performed with the MMFF94 force field (Halgren, 1996*a*,*b*,*c*,*d*, 1999) as implemented in the program *SYBYL* (Tripos, St Louis, USA). The net atomic charges of the polar atoms in MMFF94 are generally considerably larger than those in the theory-fitted DB, which also includes higher moments of the charge distribution. For example, the O atom in the COO^- group carries a net charge of −0.90, compared with −0.315 in the DB. Corresponding values for the O atom in the CONH group are −0.57 in MMFF94 and −0.175 in the DB. Full information on the MMFF94 force field can be found in the cited literature.

4.3. The SAPT-fitted interaction potentials

In a study to be reported elsewhere (Volkov, Nygren *et al.*, 2006), a new set of potential functions has been generated based on intermolecular interactions calculated using symmetry-adapted perturbation theory (SAPT) at the SAPT2 level, which is roughly equivalent to a second-order many-body perturbation calculation. SAPT is an *ab initio* method based on a perturbation expansion starting from isolated monomers (London, 1930; Arrighini, 1981; Chalasinski & Gutowski, 1988). It is valid for all intermolecular separations, which makes it possible to investigate the complete potential energy surface (Szalewicz & Jeziorski, 1979; Jeziorski *et al.*, 1994 and references cited therein). SAPT provides a conceptual framework for understanding intermolecular interactions since the interaction energy $E_{\rm int}$ is calculated as a sum of physically interpretable components,

$$E_{\rm int} = E^{(1)}_{\rm pol} + E^{(1)}_{\rm exch} + E^{(2)}_{\rm pol} + E^{(2)}_{\rm exch} + \ldots \qquad (3)$$

The first-order term $E^{(1)}_{\rm pol} \equiv E^{(1)}_{\rm es}$ is the classical electrostatic interaction energy between the unperturbed densities defined by (2). $E^{(1)}_{\rm exch}$ is the first-order exchange-repulsion energy which arises from the antisymmetrization of the product of the unperturbed functions of the monomers. Such antisymmetrization is needed to impose the correct permutational symmetry of the dimer wavefunction. The second-order polarization energy $E^{(2)}_{\rm pol}$ is the sum of classical induction and quantum-mechanical dispersion energies

$$E^{(2)}_{\rm pol} = E^{(2)}_{\rm ind} + E^{(2)}_{\rm disp}. \qquad (4)$$

The electrostatic, induction and dispersion energies are defined by the Rayleigh–Schrödinger perturbation theory. In the simplest version of SAPT, the symmetrized Rayleigh–Schrödinger (SRS) perturbation theory (Jeziorski *et al.*, 1978), $E^{(2)}_{\rm exch}$ results from the anti-symmetrization of the induction and dispersion wavefunctions. In other versions, this component can be defined in more complicated ways, but the numerical values of $E^{(2)}_{\rm exch}$ in all asymptotically correct versions of SAPT are almost identical to those given by the SRS theory (Patkowski *et al.*, 2004; Szalewicz *et al.*, 2005). The first- and second-order exchange energies are usually considered together, so that the interaction energy computed in the SAPT approach is discussed in terms of four fundamental types of interactions: electrostatic, exchange-repulsion, induction and dispersion.

Exchange-repulsion, dispersion and induction parameters were obtained as follows. In the first stage, values of $E^{(1)}_{\rm exch}$, $E^{(2)}_{\rm exch}$ $E_{\rm disp}$ and $E_{\rm ind}$ were calculated for 138 small organic molecular complexes using SAPT with the 6-31G**/DC+BS (dimer-centered basis set plus the bond functions at the midpoint of the interactions; Jeziorski *et al.*, 1994; Williams *et al.*, 1995; Bukowski *et al.*, 2003). 12 693 interatomic interactions involving H, C, N and O atoms were identified in the molecular set. In the second stage, pairwise coefficients a_{ij}, b_{ij}, c_{ij}, d_{ij} and f_{ij} for interactions between the atoms C, H, O, N in the expressions

$$\begin{aligned} E^{\rm fit}_{\rm ex\text{-}rep} &= \sum_{i=1}^{N_A}\sum_{j=1}^{N_B} a_{ij}\exp(-b_{ij}r_{ij}), \\ E^{\rm fit}_{\rm disp} &= \sum_{i=1}^{N_A}\sum_{j=1}^{N_B} \frac{c_{ij}}{r_{ij}^6}, \\ E^{\rm fit}_{\rm ind} &= \sum_{i=1}^{N_A}\sum_{j=1}^{N_B} d_{ij}\exp(-f_{ij}r_{ij}) \end{aligned} \qquad (5)$$

were obtained by fitting each of the intermolecular interaction energies obtained in the first stage of the project. R.m.s. discrepancies between the theoretical interaction energies and those from the fitted pairwise functions were 5.4, 1 and 5.6 kJ mol^{-1} for the exchange-repulsion, dispersion and induction terms, respectively. A full account of the fitting results, including those obtained with larger expansions, will be given in a subsequent publication (Volkov, Nygren *et al.*, 2006).

4.4. First-principle calculations

Theoretical calculations at the density-functional level of theory (DFT) were carried out with the *Gaussian*03 (Frisch *et al.*, 2004) suite of programs using the gradient-corrected hybrid B3LYP functional (Becke, 1988, 1993; Lee *et al.*, 1988) and 6-31G** (Hariharan & Pople, 1973) and DZP (Dunning, 1970) basis sets; the latter includes separate functions for the *s* and *p* orbitals. Basis-set superposition errors in the supermolecular calculations of the total interaction energies were corrected for with the counterpoise method (Boys & Bernardi,

2002). Intermolecular electrostatic interaction energies were evaluated from the theoretical monomer densities with a new program *SPDFG* (Volkov, King *et al.*, 2006), which uses the numerical Rys Quadrature method (Dupuis *et al.*, 1976; Rys *et al.*, 1983) for calculation of one- and two-electron Coulomb integrals.

All calculations were performed using our own Linux Beowulf-type cluster equipped with dual- and quad-processor AMD AthlonMP and Opteron nodes.

4.5. Test systems

To decrease the size of the systems studied and allow theoretical calculations for comparison, the disaccharide group of vancomycin and several phenyl rings were removed, leaving only the heptapeptide backbone (labeled in the following as vancomycin′ or van′; formula $C_{25}H_{37}N_8O_{11}$; Fig. 3), which is the part of the antibiotic that interacts directly with the substrates. While removal of the disaccharide leads to a small reduction in antimicrobial activity, practical considerations dictate its use in current computational studies (Axelsen & Li, 1998; Lee *et al.*, 2004). The geometries were based on the crystal structures.

H-atom positions, which are not reported in the crystallographic studies, were generated at idealized positions with *Weblab Viewer Pro* 4.0 (Molecular Simulations Inc., San Diego, CA, USA). The X—H bond lengths were extended to the standard neutron diffraction distances (Allen *et al.*, 1992.).

Table 2
The electrostatic interaction energies and the total intermolecular interaction energies for vancomycin fragment–substrate complexes.

Hydrogen-bond geometries are given as supplementary material. The number in the first column refers to the different molecules in the asymmetric unit.
(*a*) Electrostatic interaction energies (kJ mol^{-1}).

Complex	Reference	*Gaussian*03 B3LYP/6-31G**	*Gaussian*03 B3LYP/DZP	*SYBYL* MMFF94	DB+ EPMM
Van′–Ac	Loll *et al.* (1997)	−472	−493	−503	−516
Van′–Dlac	Loll *et al.* (1999)	−558	−582	−556	−541
Van′–AcG	Loll *et al.* (1999)	−449	−467	−503	−469
Van′1–AcDA1	Loll *et al.* (1998)	−474	−494	−554	−492
Van′2–AcDA2		−485	−505	−546	−517
Van′3–AcDA3		−468	−490	−516	−508
Van′4–AcDA4		−474	−494	−521	−506

(*b*) Total intermolecular interaction energies (kDa).

Complex	*Gaussian*03 B3LYP/6-31G**	*Gaussian*03 B3LYP/DZP	*SYBYL* MMFF94	DB+EPMM+ SAPT
Van′–Ac	−488	−488	−494	−479
Van′–Dlac	−530	−531	−594	−466
Van′–AcG	−468	−465	−478	−446
Van′1–AcDA1	−470	−467	−540	−453
Van′2–AcDA2	−467	−471	−549	−475
Van′3–AcDA3	−450	−450	−511	−465
Van′3–AcDA4	−460	−458	−517	−462

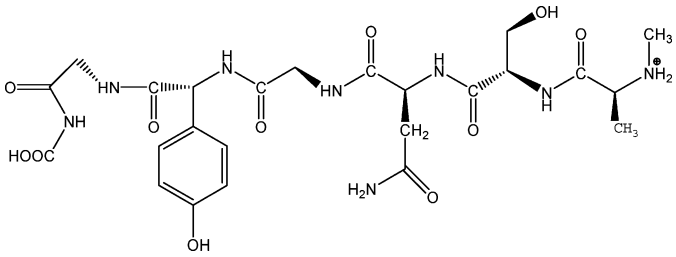

Figure 3
Schematic representation of the vancomycin fragment van′.

5. Results and discussion

5.1. The electrostatic and total interaction energies for a series of vancomycin fragment–small-ligand complexes

Seven different complexes of van′ with substituent ligands for which structural information is available (Loll *et al.*, 1997, 1998, 1999) were used in the calculations (Table 2). The electrostatic and total interaction energies from theoretical calculations with the two basis sets, from the MMFF94 force field and from the DB+EPMM+SAPT method, are compared in Tables 2(*a*) and 2(*b*), respectively. Hydrogen-bond geometries are given as supplementary material[1].

5.1.1. Electrostatic energies. The comparison of the DB+EPMM electrostatic energies with the DZP calculations is illustrated in Fig. 4. The electrostatic interaction energies are similar for the van′–Ac, van′–AcG and the four van′Ac–DAla complexes, while according to all results van′–DLac has a stronger total electrostatic interaction, in accordance with the formation of four strong hydrogen bonds.

The databank values tend to be slightly more bonding than those from the DFT calculation, with the exception of vanc′–DLac, for which the databank gives less negative values but still predicts stronger bonding than for the other complexes.

5.1.2. Total energies. The combination of the EPMM and SAPT methods allows analysis of the total interaction energies in terms of the individual components. The results show that for the complexes under consideration the exchange-repulsion contribution is cancelled to a good approximation by the dispersive and induction energies, as illustrated in Fig. 5. Thus, the total energies are close to the values from the electrostatic contributions, the differences being generally less than 10%. This result provides some justification for electrostatic only analysis of intermolecular interactions in comparable systems. The agreement of the total energies according to DB+EPMM+SAPT is poorest for the strongly bonded DLac complex, suggesting possible inaccuracies of the non-bonded

[1] Supplementary material has been deposited in the IUCr electronic archive (Reference: DZ5077). Services for accessing these data are described at the back of the journal.

potentials at short H···O distances, which will be the subject of further studies.

The numerical agreement among the theoretical results, the force-field calculation and the DB+EPMM+SAPT results are summarized in Fig. 6. The following conclusions can be drawn.

(i) The agreement between the two B3LYP calculations with different basis sets is much better for the total energy than for the electrostatic energies, suggesting that errors arising from basis-set truncation in the electrostatic energy and dispersion/repulsion/induction interactions approximately cancel each other.

(ii) The agreement between the DB+EPMM and DB+EPMM+SAPT results and DFT is of the order of 25 kJ mol^{-1}, which is about 5% of the total interaction energies of $\sim$−500 kJ mol^{-1}.

(iii) The agreement between the MMFF94 results and those from B3LYP is significantly poorer than the agreement between DB+EPMM+SAPT and B3LYP, the MMFF94 calculations generally leading to more negative energies (Fig. 7), related to the fact that the atomic charges on the polar atoms in this force field are much larger than those of the theory-fitted pseudoatoms in DB. Nevertheless, for the total energies the r.m.s. and absolute discrepancies between

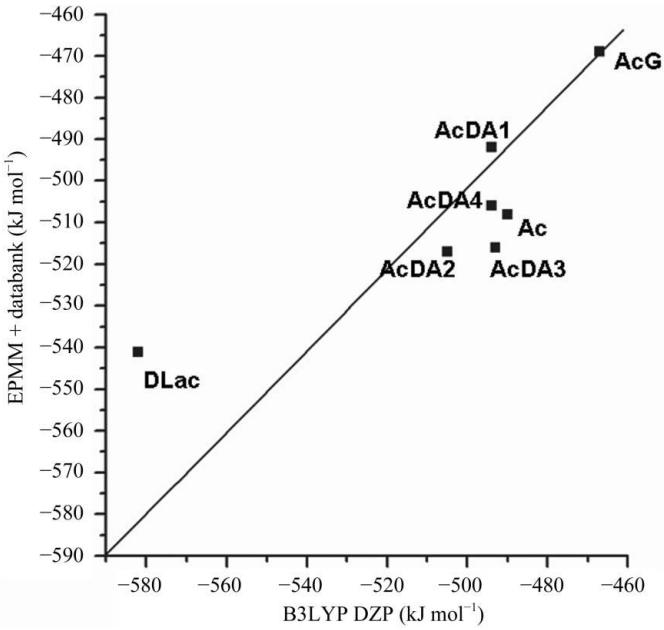

Figure 4
Comparison of calculated electrostatic energies of seven complexes of van′. The straight line represents unit slope. See text for details.

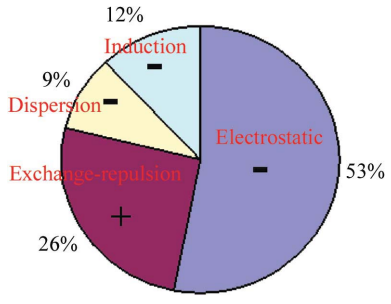

Figure 5
Relative absolute contribution of different interactions in van′ complexes as calculated by DB+EPMM+SAPT. The sign of each interaction is indicated in the corresponding segment. As shown, the induction and dispersion interactions are approximately cancelled out by the exchange-repulsion term.

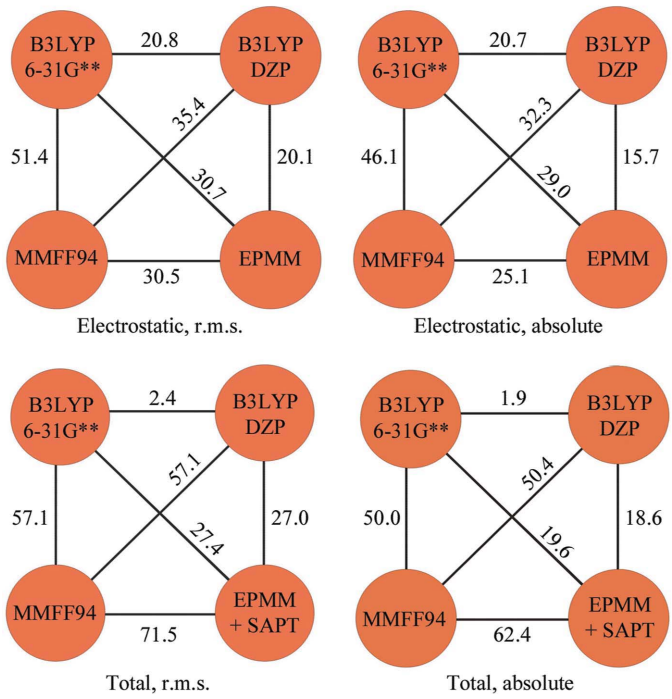

Figure 6
R.m.s. and average absolute discrepancies between first-principle, molecular-mechanics and DB+EPMM+SAPT results (from values listed in Table 2).

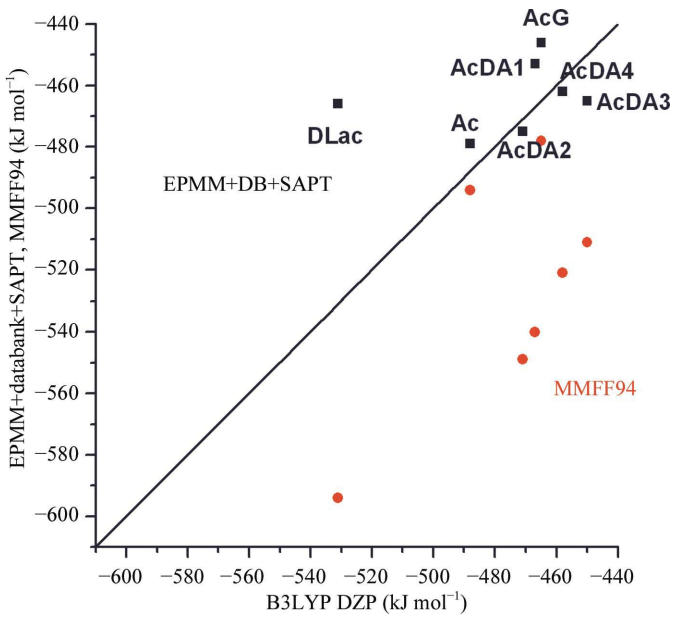

Figure 7
Comparison of DB+EPMM+SAPT and MMFF94 total energies with theory. The straight line represents unit slope.

MMFF94 and B3LYP ($\Delta_{\rm r.m.s.} \simeq 57$ kJ mol^{-1}) are larger than for the electrostatic energies ($\Delta_{\rm r.m.s.} \simeq 43$ kJ mol^{-1}), suggesting shortcomings of the non-electrostatic potential functions used in the force-field calculations.

5.1.3. Comparison with affinities measured in solution. The results may be compared with binding constants for vancomycin–small-ligand complexes in a buffered solution, which have been measured by ^{13}C NMR techniques (Loll *et al.*, 1999; Pearce *et al.*, 1995) and are summarized in Table 1. The experiments indicate the strongest complex to be formed with AcDA, a result not supported by any of our calculations performed using the crystal structure geometries. Taking the 300 M^{-1} value for the AcDA complex as a reference and a temperature of 297 K, the solution values correspond to the AcG, DLac and Ac complexes being less stable by 3–7 kJ mol^{-1}. The DFT and MMFF94 calculations indicate the DLac complex to have the lower energy, whereas DB+EPMM+SAPT predicts Ac to have the lowest total interaction energy. The calculations also show a considerable variation among the four observed AcDAl geometries of up to 25 kJ mol^{-1}, indicating that the solution values are averages over a series of conformations and may be affected by solvent effects. A similar conclusion was reached by Li *et al.* (1997) and Loll & Axelsen (2000) on the basis of simulated-annealing results.

Loll *et al.* (1999) pointed out that the loss of an intermediate hydrogen bond is only one of the factors explaining the diminished activity of vancomycin for depsipeptide ligands and that other interactions, including those that occur in the face-to-face dimer, must be taken into account. This conclusion is supported by the vancomycin-fragment calculations, which are limited to monomer–ligand complexes, but show quite a strong dependence on the geometry of the interaction even when the hydrogen bonds between the ligand and the glycopeptide fragments are of the same type (N—H···O) and number (four) as for the last five of the seven complexes listed in Table 2. It follows that other interactions play a role and therefore that cooperative effects involving interaction of the ligand with two or more molecules, as occur in the face-to-face dimer, will be of importance. Ultimately, a full quantitative understanding of the antibiotics' affinity will require precise information on the structure of the cell wall–antibiotic complex.

5.2. The interactions between balhimycin and deglucobalhimycin and cell-wall model compounds

As the DB+EPMM+SAPT results can be rapidly obtained, we have extended the calculations to complexes of balhimycin (DB+EPMM) and deglucobalhimycin (DB+EPMM and DB+EPMM+SAPT) for which structural information is available. Balhimycin is a close relative of vancomycin, differing only in the location and nature of the carbohydrate moieties. The high-resolution structures of deglucobalhimycin complexed with the dipeptide DADA and the pentapeptide L-Ala-D-Glu-γ-L-Lys-DADA and of balhimycin with DADA and the tripeptide L-Lys-DADA became available in 2002 (Lehmann *et al.*, 2002).

The complex of balhimycin with high-affinity L-Lys-DADA crystallizes with eight antibiotic molecules in the asymmetric unit (PDB code 1go6), of which only four have tripeptide-occupied receptor pockets. Two of the balhimycin molecules form a face-to-face dimer incorporating two tripeptide molecules, whereas some of the antibiotic molecules participating in the back-to-back dimers have empty binding pockets. The stability of this face-to-face dimer has been invoked to suggest a kinetic barrier to dissociation and therefore a further impediment to the crosslinking of the peptides required for cell-wall growth (Lehmann *et al.*, 2002). The DB+EPMM results explain that the antibiotic–substrate electrostatic interaction energy is significantly more stabilizing in the geometry of the face-to-face dimers than that in the back-to-back dimers, the $E_{\rm es}$ (averaged over the two similar complexes) being −373 and −314 kJ mol^{-1} for the face-to-face and back-to-back dimers, respectively (Table 3).

Deglucobalhimycin–DADA (PDB code 1hhu) crystallizes with four symmetry-equivalent moieties of the complex in the asymmetric unit. Four antibiotic molecules form two back-to-back dimers, both of which form face-to-face dimers with symmetrically related back-to-back dimers. The deglucobalhimycin interacts with the dipeptide DADA through four strong

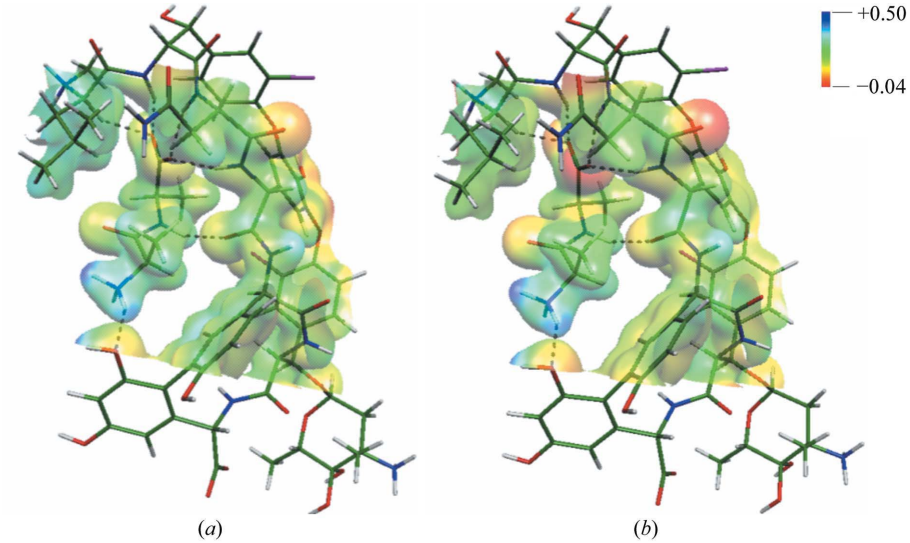

Figure 8
The electrostatic potential in the antibiotic–substrate region mapped on the 0.02 au electron-density isosurface in the deglucobalhimycin–DADA complex (*a*) according to the dataank and (*b*) according to the MMFF94 point charge model. The electrostatic potential is color coded as follows: deep red, −0.04 au; deep blue, +0.50 au; orange, yellow, green and cyan represent intermediate values as indicated on the color scale. Hydrogen bonds are indicated by dotted lines.

Table 3
The electrostatic and total interaction energies (kJ mol^{-1}) for deglucobalhimycin–substrate complexes with geometries from Lehmann *et al.* (2002).

Bal, balhimycin; Db, deglucobalhimycin. The numbering in the first column refers to the different molecules in the asymmetric unit.

Complex	E_{es}		E_{tot}	
	Data bank EPMM	MMFF94	DB+EPMM+ SAPT	MMFF94
Bal1–L-Lys-DADA	−365	−451	−346	−479
Bal2–L-Lys-DADA	−380	−474	−360	−483
Bal3–L-Lys-DADA	−302	−321	−259	−319
Bal4–L-Lys-DADA	−325	−375	−295	−380
Db1–DADA	−503	−484	−421	−465
Db2–DADA	−469	−475	−408	−481

hydrogen bonds, similar to the interactions between vancomycin and AcG (Fig. 1). The calculated electrostatic and total energies of the antibiotic–DADA complexes described by Lehmann *et al.* (2002) are summarized in Table 3. As for the vancomycin complexes, the differences between different geometries are not negligible.

In Fig. 8, the electrostatic potential in the antibiotic–substrate region of the complexes of deglucobalhimycin with the dipeptide DADA is mapped on an isodensity surface using the program *XDPROP* (Koritsanszky *et al.*, 2003) interfaced with *MOLEKEL* (Flükiger, 1992; Portmann & Lüthi, 2000). The potentials according to the multipolar density parameters from the databank and to the atomic point charges from the MMFF94 force field are qualitatively similar, but there are pronounced differences near the oxygen and nitrogen positions, where the MMFF94 potential has much larger absolute values. As the MMFF94 point charges of the polar atoms are very much larger than those of the pseudoatoms in the databank, this result is not surprising.

5.3. Energy of deglucovancomycin–substrate complexes at a theoretical geometry

In a recent study, Lee *et al.* (2004) calculated the interaction between deglucovancomycin and deglucoteicoplanin and Ac-D-Ala-D-Ala and Ac-D-Ala-D-Lac by both HF and DFT (B3LYP) methods. We have used the published geometry from the HF optimization of the deglucovancomycin complexes to calculate the energy differences of the D-Lac for D-Ala substitution with the DB+EPMM+SAPT method, keeping in mind that the parameters of this method are derived from observed and not from theoretically optimized geometries (Table 4). According to DB+EPMM, the electrostatic energy is less negative for the depsipeptide complex as expected, but in the total energy this difference is partly compensated by the other interactions. Although this effect is not reproduced by the HF calculations, it is in accordance with the observation that the change in hydrogen bonding is only one of the contributors to the different affinities of the peptide and depsipeptide ligands for the glycopeptides.

Table 4
Calculated energies (kJ mol^{-1}) for vancomycin aglycon–substrate complexes at the theoretical geometries of Lee *et al.* (2004).

	E_{es}†	E_{int}‡	E_{int}, HF	E_{int}†, DFT (B3LYP)
Vancomycin aglycon–Ac-D-Ala-D-Ala	−609	−592	−459.2	−513.4
Vancomycin aglycon–Ac-D-Ala-D-Lac	−596	−588	−438.9	−498.3
Δ	13	4	20.3	15.1

† This work, DB+EPMM, HF geometry. ‡ DB+EPMM+SAPT, HF geometry.

6. Conclusions

The DB+EPMM+SAPT method allows extension of the geometric information obtained by X-ray crystallography to energies of interaction at a level comparable to that from first-principle calculations. The results on the electrostatic and total intermolecular interaction energies of a series of complexes of glycopeptide antibiotics with small ligands, including dipeptides, a depsipeptide and a tripeptide, agree reasonably well with those of theoretical calculations at a fraction (typically 1/300–1/400 for the calculations presented) of computer time. They reveal some shortcomings of the MMFF94 force-field method, which is based on point charges rather than aspherical atomic charge distributions. A strong dependence on the geometry of the interaction is found, even when the number of hydrogen bonds between the substrate and antibiotic fragment is the same. While high-resolution X-ray data are required to obtain interaction energies at a quantitative level, the techniques developed have potential for joint X-ray/energy refinement of macromolecular structures.

Support of this work by the US National Institutes of Health through grant GM56829 (PC) and the US National Science Foundation through grants CHE0236317 (PC) and CHE0239611 (KS) is gratefully acknowledged.

References

Allen, F. H., Kennard, O., Watson, D. G., Brammer, L., Orpen, A. G. & Taylor, R. (1992). *International Tables for Crystallography*, Vol. *C*, edited by A. J. C. Wilson, pp. 685–706. Dordrecht: Kluwer Academic Publishers.
Arrighini, P. (1981). *Intermolecular Forces and Their Evaluation by Perturbation Theory*. Berlin: Springer.
Axelsen, P. H. & Li, D. (1998). *Bioorg. Med. Chem.* **6**, 877–881.
Barna, J. C. & Williams, D. H. (1984). *Annu. Rev. Microbiol.* **38**, 339–357.
Becke, A. D. (1988). *Phys. Rev. A*, **38**, 3098–3100.
Becke, A. D. (1993). *J. Chem. Phys.* **98**, 5648–5652.
Boys, S. F. & Bernardi, F. (2002). *Mol. Phys.* **100**, 65–73.
Buckingham, A. D. (1967). *Adv. Chem. Phys.* **12**, 107–142.
Bukowski, R., Cencek, W., Jankowski, P., Jeziorski, B., Jeziorska, M., Kucharski, S. A., Misquitta, A. J., Moszynski, R., Patkowski, K., Rybak, S., Szalewicz, K., Williams, H. L. & Wormer, P. E. S. (2003). *SAPT*2002: *An Ab Initio Program for Many-Body Symmetry-Adapted Perturbation Theory Calculations of Intermolecular Interaction Energies*. University of Delaware/University of Warsaw.
Chalasinski, G. & Gutowski, M. (1988). *Chem. Rev.* **88**, 943–962.
Coppens, P. (1997). *X-ray Charge Densities and Chemical Bonding*. Oxford University Press.

Dunning, T. H. Jr (1970). *J. Chem. Phys.* **53**, 2823–2833.
Dupuis, M., Rys, J. & King, H. F. (1976). *J. Chem. Phys.* **65**, 111–116.
Flükiger, P. F. (1992). Thèse No. 2561. Département de Chimie Physique, Université de Genève, Genève.
Frisch, M. J. *et al.* (2004). *Gaussian*03, Revision C.02. Gaussian Inc., Wallingford, CT, USA.
Ge, M., Chen, Z., Onishi, H. R., Kohler, J., Silver, L. L., Kerns, R., Fukuzawa, S., Thompson, C. & Kahne, D. (1999). *Science*, **284**, 507–511.
Halgren, T. A. (1996*a*). *J. Comput. Chem.* **17**, 490–519.
Halgren, T. A. (1996*b*). *J. Comput. Chem.* **17**, 520–552.
Halgren, T. A. (1996*c*). *J. Comput. Chem.* **17**, 553–615.
Halgren, T. A. (1996*d*). *J. Comput. Chem.* **17**, 616–641.
Halgren, T. A. (1999). *J. Comput. Chem.* **20**, 720–729.
Hansen, N. K. & Coppens, P. (1978). *Acta Cryst.* A**34**, 909–921.
Hariharan, P. C. & Pople, J. A. (1973). *Theor. Chim. Acta*, **28**, 213–222.
Harris, C. M., Kopecka, H. & Harris, T. M. (1983). *J. Am. Chem. Soc.* **105**, 6915–6922.
Hiramatsu, K. (1998). *Drug Resist. Updates*, **1**, 135–150.
Jeziorski, B., Szalewicz, K. & Chalasinski, G. (1978). *Int. J. Quant. Chem.* **14**, 271–287.
Jeziorski, B., Moszynski, R. & Szalewicz, K. (1994). *Chem. Rev.* **94**, 1887–1930.
Koritsanszky, T., Howard, S. T., Richter, T., Macchi, P., Volkov, A. V., Gatti, C., Mallinson, P. R., Farrugia, L. J., Su, Z. & Hansen, N. K. (2003). *XD: A Computer Program Package for Multipole Refinement and Topological Analysis of Charge Densities from Diffraction Data*. http://xd.chem.buffalo.edu/.
Lee, J. G., Sagui, C. & Roland, C. (2004). *J. Am. Chem. Soc.* **126**, 8384–8385.
Lee, C., Yang, W. & Parr, R. G. (1988). *Phys. Rev. B*, **37**, 785–789.
Lehmann, C., Bunkòczi, G., Vértesy, L. & Sheldrick, G. M. (2002). *J. Mol. Biol.* **318**, 723–732.
Levy, S. B. (1998). *Sci. Am.* **3**, 46–53.
Li, D., Sreenivasan, U. & Puga, F. J. II (1997). *J. Mol. Recognit.* **10**, 73–87.
Loll, P. J. & Axelsen, P. H. (2000). *Annu. Rev. Biophys. Biomol. Struct.* **29**, 265–289.
Loll, P. J., Bevivino, A. E., Korty, B. D. & Axelsen, P. H. (1997). *J. Am. Chem. Soc.* **119**, 1516–1522.
Loll, P. J., Kaplan, J., Selinsky, B. S. & Axelsen, P. H. (1999). *J. Med. Chem.* **42**, 4714–4719.
Loll, P. J., Miller, R., Weeks, C. M. & Axelsen, P. H. (1998). *Chem. Biol.* **5**, 293–298.
London, F. (1930). *Zeitschr. Phys.* **63**, 245–279.
McCormick, M. H., Stark, W. M., Pittenger, G. E., Pittenger, R. C. & McGuire, J. M. (1955–1956). *Antibiot. Annu.* **3**, 606–611.
Malabarba, A., Nicas, T. I. & Thompson, R. C. (1997). *Med. Res. Rev.* **17**, 69–137.
Patkowski, K., Jeziorski, B. & Szalewicz, K. (2004). *J. Chem. Phys.* **120**, 6849–6862.
Pearce, C. M., Gerhard, U. & Williams, D. H. (1995). *J. Chem. Soc. Perkins Trans. 2*, pp. 159–162.
Portmann, S. & Lüthi, H. P. (2000). *CHIMIA*, **54**, 766–769.
Reynolds, P. E. (1989). *Eur. J. Microb. Infect. Dis.* **8**, 943–950.
Roper, D. I., Huyton, T., Vagin, A. & Dodson, G. (2000). *Proc. Natl Acad. Sci. USA*, **97**, 8921–8925.
Rys, J., Dupuis, M. & King, H. F. (1983). *J. Comput. Chem.* **4**, 154–157.
Schäfer, M., Schneider, T. R. & Sheldrick, G. M. (1996). *Structure*, **4**, 1509–1515.
Sheldrick, G. M., Jones, P. G., Kennard, O., Williams, D. H. & Smith, G. A. (1978). *Nature (London)*, **271**, 223–225.
Sheldrick, G. M., Paulus, E., Vertesy, L. & Hahn, F. (1995). *Acta Cryst.* B**51**, 89–98.
Stone, A. J. (1995). *The Theory of Intermolecular Forces*, p. 106. Oxford University Press.
Szalewicz, K. & Jeziorski, B. (1979). *Mol. Phys.* **38**, 191–208.
Szalewicz, K., Patkowski, K. & Jeziorski, B. (2005). *Intermolecular Forces and Clusters II. Structure and Bonding*, Vol. 116, edited by D. J. Wales, pp. 43–117. Berlin: Springer.
Uttley, A. H. C., Collins, C. H., Naidoo, J. & George, R. C. (1988). *Lancet*, **1**, 57–58.
Volkov, A. V. & Coppens, P. (2004). *J. Comput. Chem.* **25**, 921–934.
Volkov, A. V., King, H. F. & Coppens, P. (2006). *J. Chem. Theory Comput.* **2**, 81–89.
Volkov, A. V., Li, X., Koritsanszky, T. & Coppens, P. (2004). *J. Phys. Chem.* **108**, 4283–4300.
Volkov, A. V., Nygren, C., Messerschmidt, M., Li, X. & Coppens, P. (2006). In preparation.
Volkov, A. V., Koritsanszky, T. S. & Coppens, P. (2004). *Chem. Phys. Lett.* **391**, 170–175.
Walsh, C. T., Fisher, S. L., Park, I. S., Prahalad, M. & Wu, Z. (1996). *Chem. Biol.* **3**, 21–28.
Williams, H. L., Mas, E. M., Szalewicz, K. & Jeziorski, B. (1995). *J. Chem. Phys.* **103**, 7374–7391.
Woodford, N., Johnson, A. P., Morrison, D. & Speller, D. C. (1995). *Clin. Microbiol. Rev.* **8**, 585–615.
Wright, G. D. & Walsh, C. T. (1992). *Acc. Chem. Res.* **25**, 468–473.